

Ag induced zero- and one-dimensional nanostructures on vicinal Si(111)

J. Kuntze*, A. Mugarza, J. E. Ortega

*Departamento de Física Aplicada I, Universidad del País Vasco, Plaza de Oñate 2, E-20018 San Sebastian, Spain
Donostia International Physics Center and Centro Mixto CSIC/UPV, Paseo Manuel Lardizabal 4, 20018 San Sebastian, Spain
(March 22, 2022)*

The formation of a Ag stabilized regular step lattice on vicinal Si(111) miscut towards $[11\bar{2}]$ is reported. The step bunching characteristic of the clean surface is prevented by a single-domain Si(111)-(3×1)-Ag reconstruction. The nanostructured surface is used as a template for growing one-dimensional arrays of 1 nm sized Ag quantum dots with a preferential spacing of 1.5 nm along the rows.

PACS number(s): 68.37.Ef, 81.16.Dn, 81.07.Ta, 81.07.Vb

Self-organization on crystal surfaces is a promising alternative for growing uniform nanostructures and templates with regular sizes and spacings [1]. In particular vicinal surfaces appear as natural substrates for the self-assembly of linear structures. Indeed, arrays of quantum wires and dots can be obtained by step decoration and step-flow growth [2,3]. Also one-dimensional templates can be tailored at vicinal surfaces by inducing periodic faceting with adsorbates [4,5] or simply by stabilizing single domains of atomic row structures at terraces [2,6]. The latter is the case of self-assembled (5×2) Au rows on vicinal Si(111) with small (1°) miscut, which can serve as read-writing tracks for atomic scale memories [6].

Here we investigate how surface reconstruction and morphology of Si(111) vicinals miscut towards $[11\bar{2}]$ are affected by Ag adsorption with special emphasis on nanostructure and device fabrication. We find that the (3×1)-Ag reconstruction prevents the equilibrium step bunching characteristic of the clean surface at 870 K. The system displays a regular array of monatomic steps with terraces that contain three equidistant Ag atomic chains. Further deposition of Ag at RT results in linear arrays of quantum dots nucleating in the trenches between the Ag rows.

The experiments have been performed in an UHV system (base pressure below 5×10^{-11} mbar) equipped with a commercial Omicron scanning tunneling microscope (STM) and low-energy electron diffraction (LEED). Samples were cut from n-type Si(111) wafers (0.05–0.1 Ωcm) with a 4° and 6.1° miscut towards $[11\bar{2}]$. The clean surface was prepared by direct current heating with the current flowing parallel to the step direction to prevent electromigration effects on the step distribution [7,8]. Surface temperature was monitored by an infrared pyrometer with the emissivity set to 0.4. The wafers were initially outgassed at 970 K for 1 h, followed by repeated flashing to 1500 K for a few seconds to remove the oxide layer and SiC. To produce ordered arrays of step bunches, we followed a procedure similar to the one given by Lin *et al.* [9]: flashing to 1500 K (10 s), followed by a fast (10 s) cooling to 1140 K (slightly above the (1×1) to (7×7) tran-

sition for Si(111) vicinal towards $[11\bar{2}]$ [10]) and a slow cooling (≤ 1 K/s) to 920 K, where the sample was held for a further postanneal of 30 min to allow step bunches to order. The pressure during the whole procedure never exceeded 3×10^{-10} mbar. Ag was evaporated from an e-beam source with the deposition being monitored by a flux-meter calibrated against a crystal balance. Typical evaporation rates were 0.3 ML/min. The pressure during evaporation was in the 10^{-11} mbar range.

Vicinal Si(111) surfaces miscut towards $[11\bar{2}]$ undergo spontaneous step bunching [10,11]. Figure 1(a) shows a large scale image of the clean surface with an array of bunched steps. The total periodicity of stepped bunches and flat (111) terraces reaches a self-limited size of approximately 70 ± 10 nm in agreement with previous reports [9,12,13].

Deposition of submonolayer coverages of Ag and subsequent annealing to 850–900 K leads to partial erosion of the ordered step arrays, triggered by the formation of (3×1) domains. The (3×1) structure is oriented almost exclusively along the step direction, contrary to Ag induced structures on flat Si(111), where all three domains of (3×1) are observed, usually in addition to coexisting ($\sqrt{3} \times \sqrt{3}$) and (7×7) phases [14–16].

To optimize the long-range order and to maximize the (3×1) coverage in one domain, we investigated the elementary preparation steps more closely. Figure 1(b) shows the same surface as (a) after subsequent deposition of 1 ML Ag followed by annealing to 870 K for 30 min. The Ag has desorbed and the surface has transformed to (7×7) reconstructed terraces of varying width, separated by monatomic steps which have partially coalesced to poorly defined bunches. We conclude that Ag promotes debunching of the surface upon annealing, since no debunching is observed directly after Ag deposition at RT. Since annealing above the Ag desorption temperature of 820 K [14] is needed for sufficient step mobility, the surface morphology is kinetically determined by the competing factors of Ag promoted debunching and (re-)bunching of the clean terraces after Ag desorption. Thus, in this case good long-range ordering cannot be achieved by mere Ag deposition and annealing.

To facilitate better ordering, Ag was deposited on the clean surface after rapid (≈ 100 K/s) quenching to RT from above the (1×1) to (7×7) transition temperature, minimizing the number and size of preexisting step bunches. STM images of the quenched surface prior to Ag deposition (not shown) reveal a surface morphology similar to the one in Fig. 1(b).

After deposition of approximately 0.3 ML Ag and subsequent annealing to 870 K for some 10 s, the (3×1) reconstruction is formed. Cycling this desorption/annealing sequence a few times further improves long-range order, overcoming the limitations of mass transport at this temperature. Alternatively, Ag can also be deposited at 870 K, but special care has to be taken to balance deposition and desorption rates. Figure 1(c) demonstrates the surface quality achieved by this preparation. On the mesoscopic (μm^2) scale the main part ($>90\%$) of the surface is covered by only one (3×1) domain. Only occasionally other rotational domains are found extending over only small areas. Due to the size of the electron beam in our LEED setup (2 mm), faint residues of such rotational domains are usually found in LEED images, as demonstrated in Fig. 1(d). Additionally, near the cathode and anode edges of the sample, we find residual $(\sqrt{3}\times\sqrt{3})$ or (7×7) domains, respectively. We attribute this to electromigration of Ag towards the cathode [17], since the observed distribution depends on the current direction. Heating by electron bombardment should eliminate this migration effect.

The (3×1) spots in the LEED image [Fig. 1(d)] are split due to superlattice diffraction [18]. From the splitting an average step separation of 4.2 ± 0.3 nm is derived [19], compatible with the dominant terrace width of approximately 3.8 nm observed by STM in Fig. 1(c). Incorporation of wider or narrower terraces, varying in width by multiples of the (3×1) unit cell size, accounts for the misfit of the local slope (4.7° for 3.8 nm terraces separated by single bilayer steps) to the macroscopic miscut. This leads to residual imperfections of the step lattice over large (μm^2) areas, which could eventually be overcome by matching the macroscopic miscut to preferred terrace sizes.

Another weak feature in the LEED image of Fig. 1(d) are faint streaks at $\times 2$ position along the $[11\bar{2}]$ azimuth, i.e., parallel to the step edge direction. These can be explained by high-resolution STM images: Figure 2 displays a close-up view of a few (3×1) reconstructed terraces for both filled and empty states. In the empty states image [Fig. 2(a)] ball-like features (mark "A") are located at step edges in the step down-direction. These are probably due to Si adatoms with a two nearest neighbor spacing along the step edge direction ($[\bar{1}10]$). The $\times 2$ spacing is likely the cause for a buckling of step edge atoms with the same periodicity, which show up as prominent bright rows in filled state images [Fig. 2(b)]. In the inset a single step edge row is seen with higher contrast. The difference in apparent height of alternating bright and shallow atoms along the row is 0.05 Å. We propose that the bright step edge rows and the adatom features both correspond to Si atoms rather than Ag, since upon (3×1) formation excess Si atoms from the (7×7) -phase have to be incorporated at steps [21]. The strong bias dependence of the adatoms and the nucleation of Ag on the step edge rows (see below) further support this assignment.

The marked triangles in both filled and empty states images correspond to maxima due to Si surface states in calculated STM images of the metal induced (3×1) reconstruction in the honeycomb chain-channel (HCC) model proposed by Erwin and Weitering [22]. The additional bright row seen in empty states images [Fig. 2(a)] corresponds to the metal atom position and is due to a superposition of states from Si and metal atoms. We note that Erwin and Weitering have found a distortion of the Si honeycombs for the case of Ag leading to a (6×1) symmetry in agreement with previous [14,16,21,23] works. In STM images, the nearly equilateral triangle of filled state maxima [cf. marks in Fig. 2(b)] was found to be distorted by pairing of maxima in neighboring rows. The direction of this pairing alternates in neighboring (3×1) unit cells, leading to the (6×1) periodicity. For the stepped surface, we observe the same distortion on occasional wider terraces. On the average terrace of approximately 3.8 nm width, we do not observe (6×1) formation. The small terrace size could facilitate strain relief by relaxation near steps, thus eliminating the driving force for (6×1) formation [22].

After fabrication and characterization of the stepped Ag/Si(111)- (3×1) surface, we can use this array as a template for further Ag growth. As shown recently for flat Si(111), one-dimensional arrays of Ag nanodots nucleate at RT on (3×1) -Ag reconstructed areas with a preferential spacing of $3a_0$ – $5a_0$, when $a_0=0.384$ nm is the lattice spacing along $<110>$ [24]. We find a very similar behaviour on stepped templates (Fig. 3), with uniform Ag nanodots of 1 nm diameter and 0.2 nm height nucleating in the trenches between the Ag rows in the (3×1) structure. The nearest neighbor distance is preferentially $4a_0$, with multiples up to $7a_0$ being observed. The existence of clear peaks in the distribution [Fig. 3(b)] suggests a nucleation at well defined lattice sites. Strictly one-dimensional lines of dots are found on 3.8 nm wide terraces, whereas narrower terraces prevent nucleation [arrows in Fig. 3(a)]. On wider terraces (not shown), a second line of Ag dots grows parallel to the first. The structural characteristics can thus be fine tuned by controlling the terrace size, i.e., by different macroscopic miscuts.

In addition to nanodot nucleation on the terraces, we observe nucleation on the bright step edge row of the (3×1) structure [cf. Fig. 2(b)]. The nucleated rows again are strictly one-dimensional, but the dots display a less regular shape and are less well ordered along $[\bar{1}10]$. The Ag nucleation at this sites provides further evidence that the step edge rows consist of Si atoms or dangling bonds rather than Ag-related features, since on the terraces Ag atoms preferentially adsorb on Si-related sites.

In summary, we have shown that Ag adsorption on vicinal Si(111) can be used for fabrication of ordered nanoscale arrays. The Ag induced (3×1) reconstruction stabilizes a well ordered step array on vicinal Si(111) miscut towards $[11\bar{2}]$, preventing the equilibrium step bunching characteristic of the clean surface [10]. The main terrace width changes by multiples of the (3×1)

unit cell size, 3.8 nm being the preferred width for 6° miscut samples. By matching the macroscopic miscut to the (3×1) cell size, the sample homogeneity on the μm scale may be further improved. Filled and empty states STM images of the detailed terrace structure are in accord with the previously proposed HCC model [22]. Using the (3×1) reconstructed step array as a template, one-dimensional chains of Ag nanodots can be grown, displaying a preferential nearest neighbor separation of four lattice constants along $[1\bar{1}0]$. Such dot arrays could eventually be used for future atomic scale memories, as recently proposed for $\text{Si}(111)-(5 \times 2)\text{-Au}$ [6].

Acknowledgment J. K. is supported by the Marie Curie grant HPMF-CT-1999-00280. A.M. and J.E.O. are supported by the Universidad del País Vasco (1/UPV/EHU/00057.240-EA-8078/2000).

* Corresponding author. Electronic address: kuntze@physik.uni-kiel.de

- [1] V. A. Shchukin and D. Bimberg, *Rev. Mod. Phys.* **71**, 1125 (1999).
- [2] F. J. Himpsel, T. Jung, A. Kirakosian, J.-L. Lin, D. Y. Petrovykh, H. Rauscher, and J. Viernow, *MRS bulletin* **24**, 20 (1999).
- [3] P. Gambardella, A. Dallmeyer, K. Malti, M. C. Malagoil, W. Eberhardt, K. Kern, and C. Carbone, *Nature* **416**, 301 (2002).
- [4] A. R. Bachmann, A. Mugarza, J. E. Ortega, and S. Speller, *Phys. Rev. B* **64**, 153409 (2001).
- [5] R. Hild, C. Seifert, M. Kammler, F. J. Meyer zu Heringdorf, M. Horn-von Hoegen, R. A. Zhachuk, and B. Z. Olshanetsky, *Surf. Sci.* **in press**, (2002).
- [6] R. Bennewitz, J. N. Crain, A. Kirakosian, J.-L. Lin, J. L. McChesney, D. Y. Petrovykh, and F. J. Himpsel, *arXiv:cond-mat/0204251*.
- [7] A. V. Latyshev, A. L. Aseev, A. B. Krasilnikov, and S. I. Stenin, *Surf. Sci.* **213**, 157 (1989).
- [8] K. Yagi, H. Minoda, and M. Degawa, *Surf. Sci. Rep.* **43**, 45 (2001).
- [9] J.-L. Lin, D. Y. Petrovykh, J. Viernow, F. K. Men, D. J. Seo, and F. J. Himpsel, *J. of Appl. Phys.* **84**, 255 (1998).
- [10] R. J. Phaneuf, E. D. Williams, and N. C. Bartelt, *Phys. Rev. B* **38**, 1984 (1988).
- [11] R. J. Phaneuf and E. D. Williams, *Phys. Rev. Lett.* **58**, 2563 (1987).
- [12] R. J. Phaneuf, N. C. Bartelt, and E. D. Williams, *Phys. Rev. Lett.* **67**, 2986 (1991).
- [13] F. K. Men, F. Liu, P. J. Wang, C. H. Chen, J. L. Lin, and F. J. Himpsel, *Phys. Rev. Lett.* **88**, 096105 (2002).
- [14] K. J. Wan, X. F. Lin, and J. Nogami, *Phys. Rev. B* **47**, 13700 (1993).
- [15] S. Hasegawa, X. Tong, S. Takeda, N. Sato, and T. Nagao, *Prog. Surf. Sci.* **60**, 89 (1999).
- [16] K. Sakamoto, H. Ashima, H. M. Zhang, and R. I. G.

Uhrberg, *Phys. Rev. B* **65**, 045305 (2002).

- [17] F. Shi, I. Shiraki, T. Nagao, and S. Hasegawa, *Ultramicroscopy* **85**, 23 (2000).
- [18] M. Henzler, *Appl. Phys.* **9**, 11 (1976).
- [19] The terrace width given here is derived from the maxima of beam intensities at a few energies and is not corrected for the spot profile. This could slightly overestimate the average terrace size, depending on the shape of the terrace width distribution [20].
- [20] J. Wollschläger, *Surf. Sci.* **383**, 103 (1997).
- [21] A. A. Saranin, A. V. Zotov, V. G. Lifshits, M. Katayama, and K. Oura, *Surf. Sci.* **426**, 298 (1999).
- [22] S. C. Erwin and H. H. Weiering, *Phys. Rev. Lett.* **81**, 2296 (1998).
- [23] J. M. Carpinelli and H. H. Weiering, *Surf. Sci.* **331–333**, 1015 (1995).
- [24] H. Hirayama, R. Horie, and K. Takayanagi, *Surf. Sci.* **482–485**, 1277 (2001).

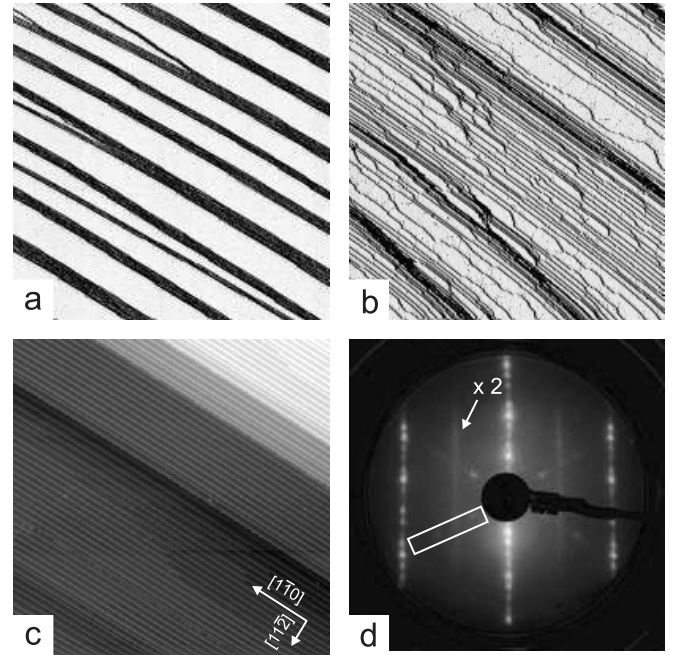


FIG. 1. (a) STM image of the clean surface. The image is differentiated to enhance the step bunches. Step-down direction is from lower left to upper right, size 600 nm. (b) (partially) debunched surface after Ag adsorption and redesorption (cf. text). Differentiation and step-down direction as in (a), size 350 nm. (c) Regular step array after (3×1) formation. Each line corresponds to a single step edge [cf. Fig. 2(b)]. Occasional multiple steps separate regular stepped regions. Step-down direction is along $[11\bar{2}]$, size 200 nm. (d) LEED pattern of the (3×1) -reconstructed surface at 26 eV. Faint residues of other rotational (3×1) domains are indicated by a box. The weak vertical stripes (arrow) are due to buckling of step edge atoms [cf. text and Fig. 2(b)].

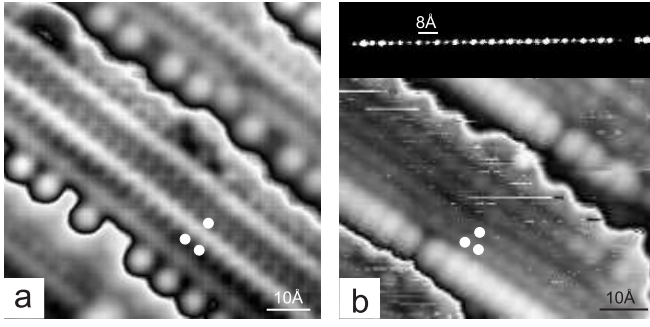


FIG. 2. High-resolution STM images of a few (3×1) reconstructed terraces. Each terrace is shown in a full grayscale for clarity. Step-down direction is from upper right to lower left. Three marks in each image indicate the position of Si related maxima in calculated STM images [22]. (a) empty state image ($U_{tip} = -1$ V, $I = 50$ pA, size 7.7 nm). The mark "A" indicates Si adatoms. The bright rows on the terrace correspond to the Ag atom sites. (b) filled state image ($U_{tip} = 1.5$ V, $I = 100$ pA, size 5 nm). The bright step edge row is probably due to Si states. It exhibits a slight buckling of 0.05 \AA (see inset, where a single row is shown with better contrast).

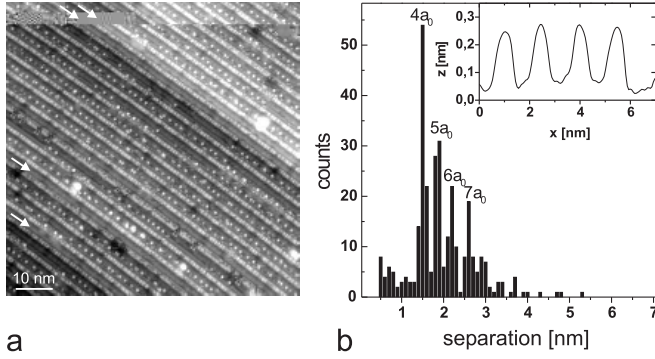


FIG. 3. (a) Array of Ag nanodots grown on a (3×1) -stabilized step lattice [cf. Fig. 1(c)] after RT deposition of approx. 0.5 ML Ag. The arrows mark terraces narrower than 3.8 nm where no dots nucleate. The distribution of the dot spacings is shown in (b). Pronounced peaks indicate preferred separations along $[\bar{1}10]$, with a clear maximum at $4a_0$ ($a_0 = 0.384$ nm). A section across four dots is seen in the inset, displaying the uniform shape of approximately 1 nm diameter and 0.2 nm height.